Application of X-ray spectroscopy to the study of electrochemically formed surface oxide films

Many analytical techniques can provide information regarding the chemical state. structure, and properties of materials. This paper focuses on two; X-ray photoelectron spectroscopy (XPS) and X-ray absorption spectroscopy (XAS), and their application to the study of electrochemically formed oxide films. A brief review of the phenomena underlying these techniques is provided, along with a description of the commonly used means for implementing them. Their capabilities and limitations are discussed, with an emphasis on the study of passive film composition and oxidation state. A summary of the behavior of Cr in oxide films on Al-Cr alloys is presented as an example. The coordinated use of both XPS and XAS is shown to be useful in achieving full understanding of materials systems such as electrochemically formed oxide films.

Introduction

Bare metal surfaces are, in general, quite reactive even when exposed to environments as benign as ambient atmospheres. The utility of common metals such as Fe, Ni, Co, Cr, and Al, in structures ranging from jet airliners to microelectronic devices, is derived from the presence of protective films which form on the metal surface at the interface with the environment. Such films, referred to as passive films, may form spontaneously upon exposure to the environment or as a result of a specific chemical or electrochemical treatment.

Because of their technological significance, the nature of passive films has been a subject of study for years. Of interest are their structure, composition, and other properties. For example, whereas the passive film on Fe is widely thought to be an oxy-hydroxide, the extent of hydration is a matter of some controversy [1]. The structure of the film is important, and some suggest that protectiveness is inversely related to the extent of crystallinity in the film. A less ordered amorphous film is

Copyright 1993 by International Business Machines Corporation. Copying in printed form for private use is permitted without payment of royalty provided that (1) each reproduction is done without alteration and (2) the Journal reference and IBM copyright notice are included on the first page. The title and abstract, but no other portions, of this paper may be copied or distributed royalty free without further permission by computer-based and other information-service systems. Permission to republish any other portion of this paper must be obtained from the Editor.

thought to have more structural flexibility. The oxidation state of the cations in the film affects the stability of the film, since the solubility is often a strong function of valence. Also, the oxidation state may increase with applied potential. Alloys are used to achieve certain functional properties, and passive films on alloys typically are enriched in some elements and depleted of others. It is very useful to know the composition of a passive film to determine which element is the source of its passivity.

In this paper, the use of X-ray spectroscopy for studying passive films on metals is described. Emphasis is placed on X-ray photoelectron spectroscopy (XPS) and X-ray absorption spectroscopy (XAS). Both can provide chemical information about a material. In the 1970s, XPS was recognized as a valuable tool for the electrochemist and was used to obtain detailed information on the chemical environment of metal deposits and the valence state of ions in surface films [2-5]. The use of XAS for electrochemical systems began somewhat later [6-9] and very recently has become more popular for such studies. In this paper, we present a summary of the phenomena on which each technique is based, followed by a description of the experimental approaches commonly used, and then a comparison of their capabilities and limitations. We focus on the study of passive film composition and oxidation state. Finally, we present data from one system to illustrate the use of each technique and the approaches to data interpretation.

Brief description of the underlying phenomena

The interaction of X-ray photons with atoms gives rise to two main phenomena which alter their propagation: scattering, leading to deflection of a photon by an atom, with or without the loss of energy, and photoionization, leading to absorption of a photon by an atom via the excitation of one or more of its electrons. The corresponding scattering and photoionization cross sections measure the probability of their occurrence. For photon energies below 10⁴ eV, the cross sections for both elastic and inelastic scattering are small, and the absorption coefficient is determined by the photoionization cross section. Both XPS and XAS use the same principle to probe matter: the absorption of X-ray photons. However, each technique focuses on different aspects of the absorption process. This section briefly describes the different aspects utilized by each technique.

Readers interested in a more detailed description of the fundamental processes in photoemission can find a very comprehensive examination in [10]. For X-ray absorption, a set of very detailed papers are cited in [11].

• X-ray photoelectron spectroscopy (XPS)
X-ray irradiation of atoms causes the emission of electrons as a result of the photoelectric effect. The emitted

electrons form a spectrum containing peaks at particular kinetic energies that represent two kinds of electrons: photoelectrons and Auger electrons. Photoelectrons arise from the interaction between a bound electron and the incident electromagnetic field. Through this interaction, the energy of the photon is imparted to the electron, which becomes unbound and leaves behind an ionized atom. A schematic view of this process is given in Figure 1(a). Auger electrons, which are discussed later, result from the subsequent de-excitation process that refills the empty orbital. The energies of both the photoemission and Auger lines are characteristic of a particular transition for each element, and this constitutes the basis for chemical identification.

In photoelectron spectroscopy, the distribution of the kinetic energies of the photoelectrons is measured. In particular, X-ray photoelectron spectroscopy refers to the use of X-rays as the exciting source. Since the energy of the photons is $h\nu$, where h is Planck's constant and ν is the frequency of the light, the principle of conservation of energy leads to

$$h\nu = E_{\epsilon}^{N-1} - E_{\epsilon}^{N} + \varepsilon_{\nu}^{\text{pe}}, \qquad (1)$$

where $\varepsilon_{\rm K}^{\rm pe}$ is the kinetic energy of the photoelectron in the continuum, and $E_{\rm i}^N$ and $E_{\rm f}^{N-1}$ are the energies of the system in the initial and final states, containing N and N-1 electrons, respectively. The binding energy, $E_{\rm B}$, of the photoelectron can be expressed as

$$E_{\rm B} = E_{\rm f}^{N-1} - E_{\rm i}^{N} = h\nu - \varepsilon_{\rm K}^{\rm pe}. \tag{2}$$

Using one-electron theory, Koopmans' theorem states that $E_{\rm B}(i)=-\varepsilon_{\rm i}$, where $\varepsilon_{\rm i}$ is the calculated one-electron orbital energy of the N-electron system [12]. Within this description the remaining (N-1) electrons are kept frozen through the photoemission process, and the only factor determining the width of the photoemission peak is the lifetime of the ionized state, in accordance with the Heisenberg uncertainty principle. This is, however, an approximation. In reality, the many-electron nature of the photoemission process has a strong effect in determining the actual binding energy, as well as producing additional spectral features such as multiplet splitting and shake-up satellites.

Multiplet splitting occurs as a consequence of the possible exchange (spin-spin) interaction between the unpaired electron left in the ionized shell and unpaired electrons in the valence levels, leading to a multiplicity of possible final states. Since the difference in energy between the different possible final states is generally small, the multiplet splitting results in the formation of broader peaks or satellite features near the main line.

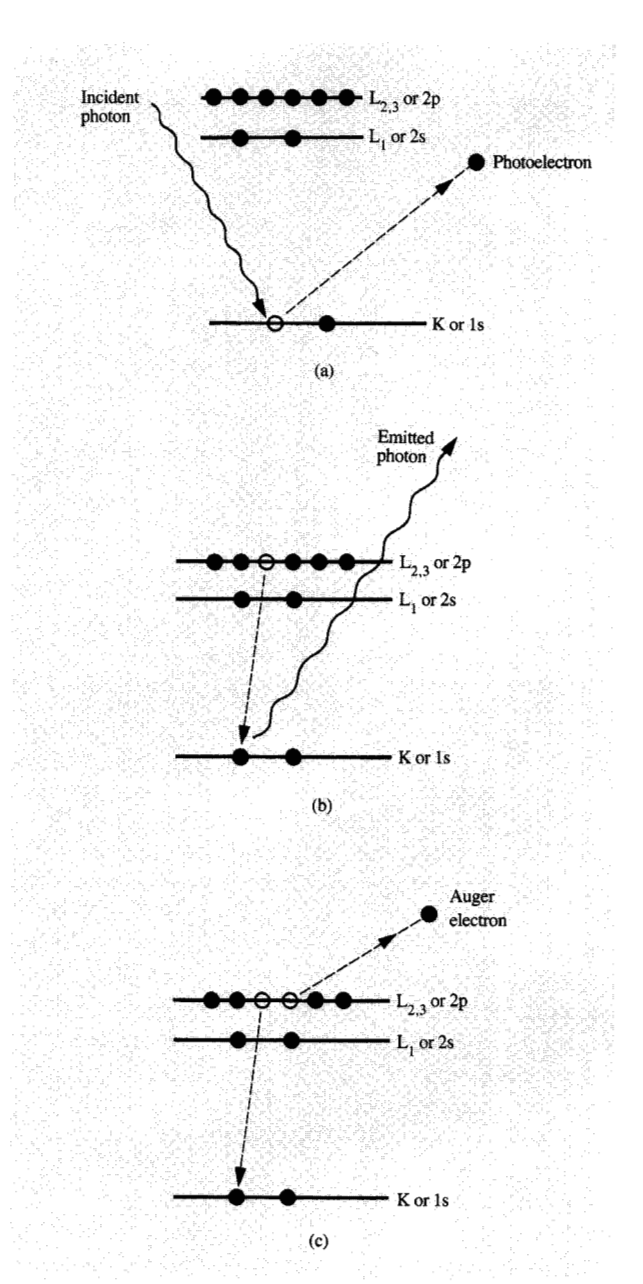
The fact that the remaining electrons do not stay frozen during photoionization, but rather adjust to the altered potential resulting from the hole that is produced, induces additional final state effects. This adjustment, denoted as relaxation, tends to screen the positive charge represented by the hole. As a result, the energy of the lowest-energy state of the system of N-1 electrons is lowered, producing photoelectrons with a higher kinetic energy than those expected if the binding energies were estimated by Koopmans' theorem. Relaxation may include not only contributions from the ionized atom but also those from the surrounding atoms in the case of molecules or condensed matter.

The state of the system does not always terminate in a single final configuration after emission of the photoelectron. A multiplicity of possible final configurations arise from the fact that excitations created simultaneously with the core ionization are allowed in the sudden approximation [13] used to calculate the transition probabilities. Consequently, the resulting photoelectrons may have their available kinetic energy lowered or raised by discrete amounts (shake-up or shake-down processes, respectively), producing satellite peaks or broadening the spectral lines.

The initial state for Auger transitions, which produce the second set of spectral lines seen in XPS spectra, is the final state of the atom after photoemission. Following ionization, the ion tends to restore its ground state, and the core hole is filled by an electronic transition from an outerlying level. The excess energy created by this transition can be used to generate a photon of that energy (fluorescence), or can be given to another electron that is emitted (Auger electron). Figure 1(b) and Figure 1(c) schematically show the fluorescence and Auger processes. The relative probability for relaxation via Auger electron emission or fluorescence depends on the atomic number Z. For Z < 30, Auger electron emission dominates. The Auger transitions are described by the one-electron energy levels using the basis set given by the j-j coupling [14]: States with quantum number $n = 1, 2, 3, \cdots$ are designated as K, L, M, ..., respectively. A transition involving an initial hole in the A shell, subsequently filled by an electron from the B shell, and resulting in an emitted Auger electron from the C shell, is designated as an ABC transition. As opposed to photoelectrons, the energy of Auger electrons is not directly dependent on the energy of the incident X-ray photons. For the transition described above, the energy of an Auger electron that is emitted as a result of the ABC transition is given by

$$E_{ABC} = E_A - E_B - E_C - U(BC) - R(BC) - E_R(C),$$
 (3)

where $E_{\rm A}$, $E_{\rm B}$, and $E_{\rm C}$ are the binding energies of an electron in the A, B, and C shells, respectively; $U({\rm BC})$ is the Coulomb interaction of the two holes in the final state; $R({\rm BC})$ is the "static" relaxation energy, the amount of energy by which the C shell has been decreased because of the presence of a hole in the B shell; and $E_{\rm p}({\rm C})$ is the



a feltifa i

Schematic representations of (a) photoionization of an electron from a core shell, (b) refilling of the hole thus created by fluorescence, and (c) refilling of the hole by an Auger transition.

"dynamic" relaxation term, similar to that described above for photoelectrons. Because Auger transitions involve the presence of two holes in the corresponding final state, the energy of an Auger electron is more strongly affected by relaxation effects than is that of a photoelectron.



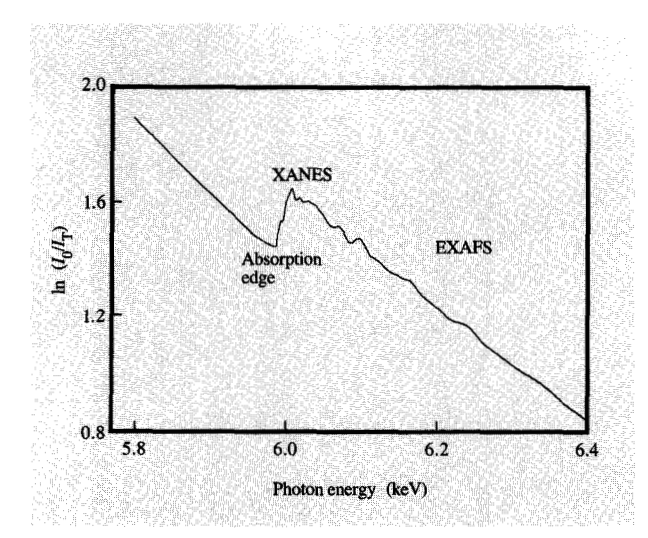


Figure /

X-ray absorption in a Cr foil, expressed as the logarithm of incident to transmitted intensities vs. photon energy.

The technique known as Auger electron spectroscopy (AES) makes use of Auger emission following radiation by an electron beam for surface elemental determination. AES is particularly useful for applications requiring fast data acquisition and high spatial resolution. However, the high background resulting from secondary electron emission degrades the signal quality; differentiation of the signal is often used to improve sensitivity. The subtle changes of Auger peaks that result from different valence states often cannot be resolved in differentiated signals, and AES is not commonly used for detailed studies of the chemical state at a surface.

So far we have discussed the basic aspects of the response of a many-electron system to the photoionization of an atom. Interaction of electromagnetic radiation with condensed matter introduces additional effects in initial and final states that result in energy shifts for both the photoelectron and Auger peaks. Initial-state effects include the change in the orbital energies of a given element with oxidation state and can be explained using a simple electrostatic model proposed by Siegbahn [15]. The binding energy generally increases with the oxidation state, which is a direct representation of the electron transfer to the ligand. However, in cases where extra-atomic relaxation is important, final-state effects may alter the trend of binding energy increase with oxidation state, complicating chemical analysis. For instance, Cu⁰ and Cu¹⁺ exhibit the same binding energy in their core photoemission peaks despite being in different oxidation states [16]. The uncertainty can only be dispelled by the Auger LVV line,

which is sensitive to the different oxidation states because of the importance of the static relaxation term in determining the energy of the Auger electrons. Auger CVV transitions, where C indicates a core level and V the valence level, are very sensitive to the local chemical environment of the central atom. The local character is given by the matrix elements I_{ij} , responsible for the Auger transition:

$$I_{ii} = |\langle \psi_i \psi_i | e^2 / r_{ii} | \psi_C \psi_i \rangle|^2, \tag{4}$$

where ψ_i and ψ_j represent the wave functions of the outerlying electrons that generate the transition via interaction with the Coulomb potential e^2/r_{ij} ; ψ_C represents the core wave function; and ψ_k indicates the outgoing Auger electron with wave number k. Because ψ_C is very localized in space, the integral involved in the above expression vanishes everywhere except in the vicinity of the central atom. Therefore, only local valence-band electrons, which are responsible for the bonding, contribute to the Auger intensity. This is in contrast to valence-band photoemission, for which contributions associated with particular elements are more difficult to assess.

Another important feature of the Auger electrons and photoelectrons emitted by a solid upon irradiation is the fact that they arise from a region only tens of Å from the surface of the sample. This is because of the limited mean free path of electrons in the 20–2500-eV kinetic energy range. These electrons interact strongly with the sample, and lose energy through plasmon excitations, core ionization, or interband excitations. As the emitted electrons lose energy, they contribute to the background instead of intensity of the spectral lines. Since the energy loss resulting from scattering of the electrons with the lattice is very small compared to the natural width of the photoelectrons and Auger lines, the yield is not affected by the temperature of the sample.

• X-ray absorption spectroscopy (XAS)

Whereas in XPS the focus is on an energy balance used to deduce the electronic structure of the initial state, in XAS the focus is on the variation of the absorption cross section associated with electronic transitions from atomic core levels to unoccupied final states as a function of X-ray energy. From perturbation theory it follows that the absorption cross section is governed by the transition probability, σ , between the initial and final states. Generally, the matrix element is calculated using the dipole approximation, and σ is given by

$$\sigma \simeq |\langle f | \mathbf{r} \cdot \hat{\mathbf{e}} | i \rangle|^2, \tag{5}$$

where \mathbf{r} is the position operator, $\hat{\mathbf{e}}$ is the unit vector corresponding to the polarization of the light, and i and f denote initial and final electron states.

As the energy of the X-rays increases, the absorption cross section generally decreases until a critical energy is reached, at which an abrupt jump occurs, as shown in Figure 2. This discontinuity (designated as the absorption edge) corresponds to the opening of the channel for the excitation of a core-level electron to an unoccupied state. A further increase in energy causes a gradual decrease in the absorption until another edge associated with a higher core level is reached.

The physical origin of the absorption spectrum in the energy range within 10 eV of the edge is caused primarily by transitions in which both the initial and final states are discrete. The possible final states depend upon the physical nature of the system: Rydberg series in single atoms, bound valence states in molecules, core excitons in ionic crystals, and unoccupied local electronic states in metals and insulators. Transitions into the continuum constitute the photoelectric effect, and produce an absorption cross section that slowly decreases with energy. The X-ray absorption decreases in this region because the probability of interaction with the nucleus decreases as the momentum transfer increases. The trend is modulated by oscillations in the absorption spectra produced by scattering of the outgoing photoelectron in the continuum with atoms surrounding the central ion. This effect is the basis of techniques referred to as EXAFS (extended X-ray absorption fine structure) and XANES (X-ray absorption near edge structure), which can be used to probe the local atomic structure surrounding the central ion.

Absorption spectra having a shape similar to that shown in Figure 2 are typically observed. Three regions can be defined:

- The edge (or threshold) region, within ±10 eV of the absorption edge.
- 2. The region of multiple scattering in the continuum, or XANES region, 5-60 eV above the absorption edge.
- 3. The region of single scattering, or EXAFS region, 40-600 eV above the absorption edge.

The indicated energy regions should be regarded as approximations.

The edge structure in condensed matter reflects the complexity imposed by the band structure compared to the discrete energy levels of isolated atoms. In metals, the core hole is fully screened by the valence electrons, and the photoelectron/core-hole interaction is negligible. Therefore, the edge region of the spectrum maps the initial unoccupied one-electron density of states. Because of the selection rules that apply, the chosen edge selects the angular momentum of the unoccupied local density of states. This has a strong influence, for instance, in the K edge of transition metals which exhibit a varying degree of

p-d hybridization. In zero order, the unoccupied bands are d bands and should not result in significant absorption. Therefore, the actual edge height measures the degree of p-d hybridization.

In insulators, the continuum threshold E_0 is the photon energy required to excite core electrons to the bottom of the conduction band, with restrictions imposed by selection rules. Generally, the density of states at the continuum threshold tends to be low, and there is no specific feature that allows identification of E_0 , which in many cases depends strongly on final-state hybridization [17]. Therefore, it is difficult to establish a direct relationship between the shift in the absorption edge and the effective charge of the ion. However, for the K edge in transition metal compounds, the rising absorption edge shifts monotonically with the valence state, and the edge position is often compared with those of standard compounds in order to assess the oxidation state. Therefore, the position of the edge is a useful parameter, making XAS useful for chemical analysis.

In insulators, the final state of the multielectron system does not produce a fully screened core hole, and therefore the Coulomb interaction modifies the states that can be occupied by a photoelectron, compared with the initial empty states. Because of the localized character of the core hole, the Coulomb attraction acts only on the local components of the unoccupied wave function, and the localized orbitals are pulled below the continuum threshold. This produces "bound excited states" or "core excitons" which probe the local structure of the system in the final state and result in peaks in the edge region. The connection between these core excitons and the structure of the unoccupied levels in the initial state depends on the insulator under consideration. For large bandgap insulators, with delocalized conduction bands, the final state of the core excitons can be described by molecular orbital calculations using a cluster formed by the ion involved and its first neighbors. However, these results are not directly related to the initial states.

In contrast, in systems for which localized molecular orbitals are associated with the bottom of the unoccupied conduction band, such as transition-metal compounds, the initial-state orbitals are pulled down rigidly by the Coulomb term, and the core excitons can be associated with the ground-state orbitals. In transition-metal compounds, the pre-edge core excitons can be classified according to the symmetry of the 3d-derived molecular orbitals of the clusters. Octahedral coordination yields t_{2g} and e_g orbitals [18] of mostly d character. These orbitals produce weak excitons at the K edge because they are dipole-forbidden transitions, whereas very strong peaks appear at the L_3 edge. Tetrahedral coordination, on the other hand, yields a_1 and t_2 orbitals. The t_2 orbitals have a partial p character because of the mixing of the d orbitals

of the metal with the p orbitals of the ligand, and they lack a center of inversion. Therefore, a dipole transition is allowed, and strong pre-edge peaks appear. An example of such a transition and the resulting usefulness for chemical analysis is discussed later in the paper.

The XANES region extends over an energy range of a few tens of eV above the absorption edge. In this energy range, an emitted photoelectron has enough kinetic energy to be considered in the continuum. However, its wavelength is large compared to interatomic distances. In this regime, it experiences strong elastic scattering by atoms in both the first and second shells surrounding the central atom. Therefore, its outgoing wavefunction, and thus the associated absorption coefficient, are modulated by interference produced by multiple scattering events within the central cluster. This interference determines the XANES oscillations. As a result of the multiple scattering, the oscillations carry information not only on the distance to atoms in the first shell, but also on distribution of atoms in the cluster. Because of the limited range of the XANES region, high resolution is needed to convert the information carried by the oscillations in k space into the interatomic distances and angles of the cluster. Furthermore, calculations to extract this information from first principles are very complex.

The EXAFS region extends from about 40 eV to about 600–800 eV above the absorption edge. This range is not always readily attainable because of possible interference from features of other absorption edges, associated with the same element or others in the compound under study. The oscillations are very weak, and require a very good signal-to-noise ratio for detection. This is compensated in part by low resolution requirements, given the large energy range available. In the EXAFS regime, the photoelectrons have a higher kinetic energy and are less likely to be elastically scattered. Therefore, the weak oscillations arise from single scattering events and carry information regarding only average distance to the first coordination shell around the central atom, not information regarding bonding angles.

In this paper, we focus on the edge region and its connection with the oxidation state of electrochemically formed films.

Experimental techniques and requirements

• X-ray photoelectron spectroscopy

Systems for XPS analysis are commercially available, and descriptions of them and associated experimental techniques may be found in several sources [19, 20]. Accordingly, we describe them only briefly.

XPS is carried out in ultra-high vacuum (UHV, about 10^{-10} torr), primarily to avoid contamination of the surface of the sample under investigation. Lab-scale X-ray sources

are available, and the most intense beams are generated by Al or Mg sources. It is common to make use of dual anodes to aid in fingerprinting unknowns, since Auger lines are independent of the source energy, whereas XPS lines shift position. Monochromators are often used to select the energy distribution of the X-ray beam in order to eliminate either the $K\alpha$ or $K\beta$ component and also the Bremsstrahlung radiation, which increases the background.

The emitted electrons are detected by one of two types of spectrometers: cylindrical mirror or concentric. The latter type has better resolution, typically better than 100 meV. However, for standard XPS measurements, the resolution is limited by the source. Detailed descriptions of the two types of spectrometers may be found in [19]. As a result of the matrix element described above, electrons from orbitals with quantum numbers $\ell > 0$ are not emitted isotropically. Therefore, the number of electrons collected by the spectrometer depends on the angle between the spectrometer and the incident radiation.

Since XPS is an ex situ technique, care must be taken to minimize changes to the surface of the sample prior to introduction into the UHV environment. It is possible to build a chamber for electrochemical treatment directly onto a port of the system so that the sample is exposed only to an inert environment after it is removed from the electrolyte [21, 22]. However, such care may not be sufficient to prevent alteration, e.g., of the very reactive surfaces of some bare metals which may oxidize during transfer even in a nominally inert gas.

Once the sample is in the instrument and aligned in the path of the beam, data are collected over a given electron energy range. Counting typically takes place during many cycles to improve the signal-to-noise ratio. Data are obtained over several energy ranges in order to monitor many different elements. A large computer-based database exists that compiles a large number of published binding and Auger energies for most elements and their compounds [23]. The interpretation of the data obtained is greatly facilitated by comparison with previously published literature.

• X-ray absorption spectroscopy

In contrast to XPS, a wider range of experimental arrangements is possible in XAS, and therefore we discuss them to a greater extent. Several excellent reviews present more detail [11, 24, 25]. In XAS, the absorption of the X-rays is measured as a function of the energy of the incident beam; the energy is monotonically varied via a monochromator. At 1 keV, the typical energy resolution needed is of the order of 1 eV. In order to have sufficient flux at each energy to generate a signal that will allow an analysis to be carried out in a reasonable amount of time, the nonmonochromatized beam must be relatively intense. This necessitates the use of radiation produced by a

synchrotron light source, of which only a few currently exist in the U.S. A synchrotron consists of a large vacuum ring through which high-energy electrons are accelerated by magnets. At every bend of the synchrotron, a high flux of coherent photons is tangentially emitted over a large range of energies. Beryllium windows permit the X-rays to be extracted from the ring to separate beam lines.

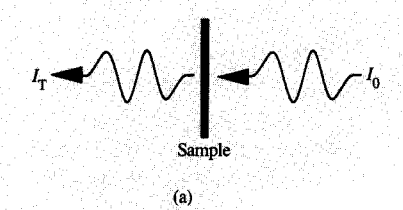
Several different experimental arrangements have been used in XAS studies. A few are shown schematically in Figure 3. The most common arrangement involves measurement of X-ray absorption in transmission, as in part (a). A sample is placed in the path of the beam, and the absorption is given by

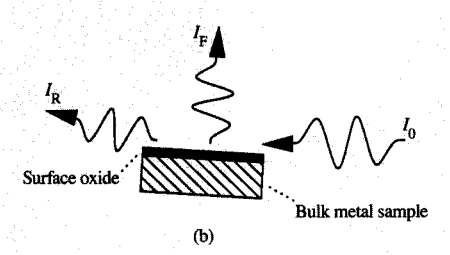
$$\mu x = \ln\left(\frac{I_0}{I_T}\right),\tag{6}$$

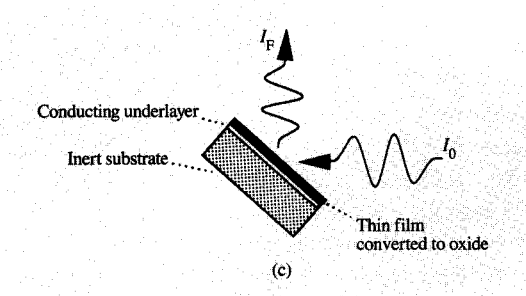
where μ is the linear absorption coefficient, x is the sample thickness, and I_0 and I_T are the incident and transmitted beam intensities, respectively. In this approach, the beam intensities are usually measured with gas ionization chambers placed in the path of the beam to either side of the sample. Ionization by the beam of the gaseous environment in an ionization chamber results in a current flow between two charged plates, the magnitude of which is proportional to the intensity of the beam. In order to generate a significant decrease in the transmitted intensity, a concentrated sample of the order of an absorption length thickness is required. This approach is obviously not useful for the study of thin surface oxide films. As for XPS data, XAS edge spectra are commonly analyzed by comparison to reference standards. These reference standards are usually transmission data from known powder or foil samples.

For dilute or very thin samples, better sensitivity is achieved by detecting the absorption via fluorescence. As described above, there is a certain probability that the photo-ionized state will relax by the emission of radiation; this radiation can be detected at a position out of the direct beam path, improving considerably the signal-to-noise ratio. For thin or dilute samples, the absorption is linearly proportional to the fluorescence produced [26], and the absorption coefficient can therefore be determined by the ratio of the fluorescent to incident beam intensities.

Surface sensitivity, a requirement for the study of passive oxide films, may be achieved by several means. One technique uses glancing-angle geometry, as shown in part (b) of Figure 3. Total external reflection of X-rays will occur for very smooth surfaces and incident angles less than a critical angle. A recent calculation has shown that the penetration depth (the depth at which the intensity is reduced by a factor of 1/e) for 6-keV X-rays (close to the Cr K edge) in Al_2O_3 is a few nm for incident angles less than 5 mrad [24]. At the critical angle of about 6 mrad, the







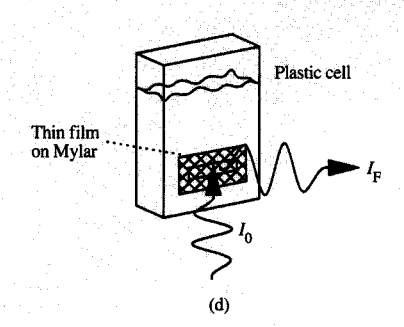


Figure 3

Schematic representations of various experimental configurations used in XAS studies: (a) transmission configuration, (b) glancing-angle configuration, (c) configuration for examination of a thinfilm sample on a metallized, inert substrate, and (d) configuration for examination of a thin-film sample on a Mylar (window) substrate.

X-ray penetration quickly increases to hundreds of nm, which may be considered to be the bulk of the sample. Therefore, it is possible to study thin surface films using a

glancing-angle geometry with a detector placed above the sample to measure fluorescence. For *in situ* analysis, the treatment is carried out in a large volume of electrolyte contained by a thin polymer membrane such as a Mylar sheet. Most of the electrolyte is then withdrawn to leave a thin liquid layer beneath the polymer film. This approach is difficult in a glancing-angle configuration because the apparatus tends to interfere with the path of the beam. Furthermore, the current distribution and mass transport for electrochemical cells with a thin electrolyte layer are poor, resulting in unsatisfactory electrochemical control of the surface.

Another approach that can be used for surface sensitivity is to eliminate the bulk of the material from which an oxide film is formed by depositing a thin film of the material onto an inert substrate covered with a thin conducting layer of Au, Nb, or Ta, as in part (c) of Figure 3. Upon electrochemical polarization, the thin film is converted totally into an oxide. With this technique, the beam is typically incident on the sample at an angle of 45°, and the fluorescent X-rays are detected at 90° to the incident beam.

A technique that facilitates surface sensitivity and *in situ* measurements with good electrochemical control has been developed recently [27], and is depicted in part (d) of Figure 3. A thin film is deposited onto a Mylar substrate coated with a thin conducting layer of Au, Nb, or Ta. The sample seals a hole in an electrochemical cell to form a window; in this fashion the cell can contain a large volume of electrolyte and reference and counter electrodes. X-rays incident on the sample at 45° pass through the Mylar and conducting layer to reach the thin film of interest. Fluorescent X-rays pass through the substrate to a detector. Noise associated with the scattering of the incident beam by the electrolyte necessitates the use of an energy-discriminating solid-state detector that samples only the energy range around the $K\alpha$ radiation.

The use of XAS to determine composition and valence is fairly straightforward. The beamline monochromator is adjusted to pass X-rays in the range of the absorption edge of interest. The beam, sample, and detector are aligned so that the proper area is illuminated at the correct angle. The monochromator motor is then programmed to scan the energy range from about -50 eV to +200 eV with respect to the energy of the edge. Typically, step sizes are smaller in the region near the edge in order to resolve edge features. The regions ahead of and beyond the edge are useful for background subtraction and edge height determination. If the sample is not moved or if the beam footprint on the sample is reproducible, the height of the absorption edge may be used to quantify the amount of the given element under study. Periodic energy scans on reference standards are carried out in order to monitor possible monochromator shifts.

In order to study a different element in the compound or system under study, it is necessary to slew the monochromator over a large range to reach the energy associated with the edge of interest. Following any such major adjustment, the beam may need to be realigned and recalibrated. As a result, it is not simple to collect data for several elements in a dynamic system such as a surface under electrochemical control.

Capabilities and limitations of XPS and XAS

In this section we briefly discuss the comparative capabilities and limitations of XPS and XAS. Again, the emphasis is on the use of these techniques for the investigation of the oxidation state of thin electrochemically formed surface oxide films.

As discussed earlier, photoelectrons and Auger electrons are sensitive to the chemical environment and have a short mean free path in solids. As a result, XPS is well suited for the study of the chemical state of very thin films. As a rule of thumb, the mean free path for the most energetic photoelectrons (valence electrons) that can be excited with an Al K α source (\approx 1480 eV) ranges from 10 to 20 Å for metals and 20 to 40 Å for oxides [20]. However, not many have been directly measured for oxides. For deeper core levels, the mean free path decreases and can be as low as 5 Å. Since the attenuation is exponential, it is possible in some cases to study the kinetics of film formation by monitoring the evolution (vs. some relevant parameter) of the intensities of the photoelectron peaks arising from the film and the underlying metal. Because of the capabilities of electron analyzers, large portions of the electron spectrum can be examined. Information can thus be obtained over many energy ranges for all the elements of a system except hydrogen and helium. These elements are difficult to detect by XPS because of their comparatively low photoionization cross sections. It is also possible to assess the depth distribution of elements and their oxidation state. The escape depth of photoelectrons increases with their kinetic energy, and different peaks associated with a given element are often found over a wide range of energy. The relative intensity of these peaks is thus affected by the depth below the surface from which the signal originates. Furthermore, the signal from the near-surface region can be enhanced by detecting photoelectrons emitted at a more glancing angle (by rotation of the sample). The comparison of a number of peaks from spectra taken at different angles provides considerable information on depth distribution.

Because the kinetic energies of the core photoelectrons and Auger electrons have a rather direct relation with the oxidation state of the central atom, XPS is well suited for the study of charge transfer in the initial state and of final-state relaxation effects. In thin oxide films, the study of the final-state satellites may be of greater importance than a

precise determination of the binding energy in assessing the chemical state of the films, because the underlying metal may affect the energy peak positions, causing them to differ from bulk standards. In general, the need for a meaningful reference level for energy determination is one of the limitations of XPS, as discussed next.

In XPS instruments, the sample is electrically connected to the spectrometer so that their Fermi levels are equivalent if the sample is metallic. Since the photoelectron kinetic energy is measured with respect to the Fermi level of the spectrometer, the work function of the spectrometer is taken into account for determination of the photoelectron binding energy. Sometimes equilibrium cannot be achieved between the spectrometer and insulating samples, however, causing the sample potential to remain electrically floating. The emission of photoelectrons then leads to the accumulation of positive charge and to an offset in the photoemission and Auger peak energies. In the case of very thin films such as electrochemically formed oxides which are typically a few nm thick, equilibrium can generally be reached by the flow of charge into the films. However, the flow of charge is regulated by the position at which the Fermi level is pinned at the interface. This leads to the creation of an interfacial dipole that bends the energy bands in the insulator. Therefore, the use of the signals from the substrate as an energy reference yields values that may depend on the thickness and interfacial properties of the film. Sometimes the C 1s signal from adventitious carbon (hydrocarbons, etc.) can be used as a reference. However, this should be done with caution, since it is not a very precise method [28] and requires some knowledge of the kind of carbon species present and the effect of the surrounding potential on the C levels. Also, final-state effects in very thin insulating films may differ from those from the bulk form of the same compound. This can be particularly important at the metal-insulator interface, where the metallic phase strongly influences relaxation effects.

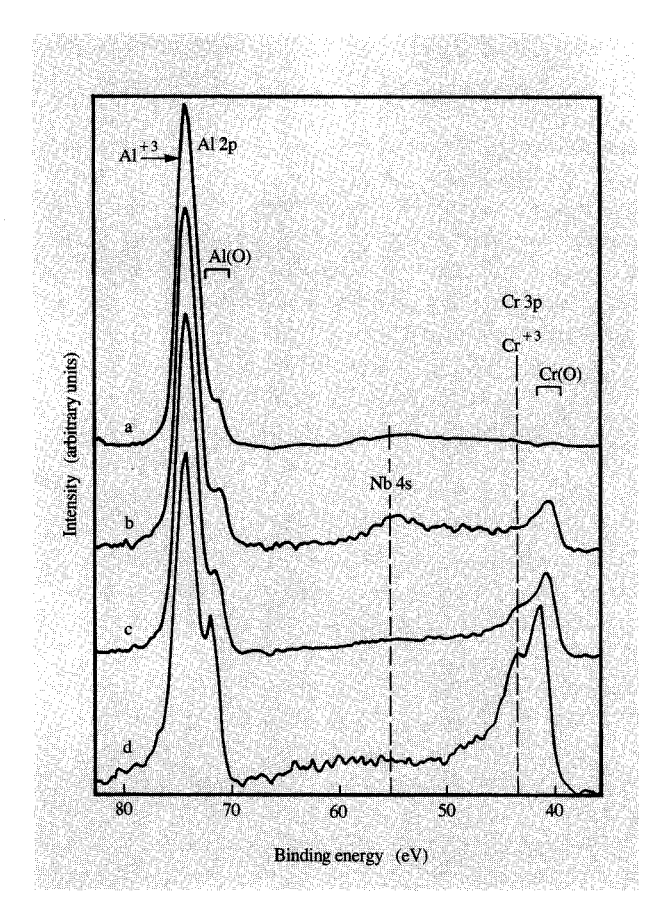
As a result of these difficulties, the study of the chemical state of very thin films may seem a hopeless task. However, the rich array of responses from a particular film provides many clues which lead the researcher to the properties of such films. A helpful phenomenon, discussed above, is the appearance of satellite peaks. These peaks depend strongly on the nature of the final states, which themselves depend on the nature and spatial arrangement of the bonding structure. For late transition-metal compounds, the satellite structure has been associated mostly with final states with different charge transfer from the ligand. This effect is also believed to have a strong influence on the line shape of the LVV Auger emission, as discussed later. For earlier transition-metal compounds, the satellite structure seems more directly related to final excited states in the ligand [29].

Electrochemically prepared surfaces that are not rinsed with water prior to analysis may carry a residue of the double layer associated with the electrochemical polarization. The adsorbed ions comprise a dipole that can generate a strong electrostatic field and influence XPS measurements. There are several examples in the literature in which the binding energies of electron orbitals in metals deposited under different potentials are shifted [30]. This is not an indication of a different chemical environment in the film. Rather, it results from different degrees of pinning to the potential in the electrolyte, which remain because of the persistence of the double layer in UHV conditions, at least through the duration of the experiment. This could be interpreted as a drawback or an advantage, depending on the focus of the particular study.

Finally, XPS is a very versatile and low-cost method. At present, there exist entry locks that permit rapid introduction of samples into a UHV chamber, either from air or from a better-controlled environment [21, 22]. However, the extent to which the UHV environment required for XPS may be detrimental to an electrochemically prepared film has been and continues to be a subject of study [30–32].

Given the capabilities of XPS, it is reasonable to question the need for leaving one's own laboratory to carry out synchrotron-based experiments. Probably the most pertinent feature of XAS edge experiments in connection with the study of electrochemically formed thin films is that such experiments can be carried out either in an ambient environment or in situ in an electrochemical cell. This eliminates possible spurious artifacts that may arise during emersion and transfer to a UHV chamber. Furthermore, since the edge region can be monitored very quickly, the time evolution of a system can be studied with XAS. Regarding surface oxides, the kinetics of film formation and dissolution can thus be monitored. Unfortunately, only the time evolution for absorption edges close in energy can be monitored during a run. This can complicate the study of oxide films on alloys, where compositional effects may be relevant to the passivating properties of the film. To compensate for this limitation, absorption experiments offer the possibility of carrying out structural measurements in very thin films with only shortrange order. This is accomplished by detailed XANES and EXAFS analysis. Because data acquisition for these techniques requires a considerable amount of time, this is usually done only at the initial and final stages of an electrochemical experiment.

Another severe limitation of *in situ* XAS measurements on electrochemically formed films is given by the constraints imposed by the synchrotron radiation. Because soft X-rays cannot pass through the beryllium windows that separate the vacuum in the storage ring from the atmosphere in the experimental chamber, the edges of light



Eigina /

XPS spectra for as-deposited 40-Å-thick Al films having bulk compositions of 5%, 20%, 32%, and 43% Cr, as shown by curves a-d, respectively. The spectra were normalized to the height of the Al⁺³ peak. From [33], reprinted by permission of the publisher, The Electrochemical Society, Inc.

elements cannot be reached. Thus, light elements can be studied only in vacuum conditions, without the beryllium window present.

Notwithstanding the limitations described above, XAS is a very useful tool for studying electrochemically formed films, and offers the possibility of performing both *in situ* and *ex situ* measurements on the same material system. Results from *in situ* and *ex situ* experiments on passive films are not always in accord with each other [31, 32]; assessing the sources of the discrepancies may be crucial for understanding the properties of the films. Since *ex situ* XAS results can be directly compared to those of XPS measurements, the two techniques complement each other. Therefore, probing the same system with both techniques is a very useful approach for the study of passive films formed under electrochemical control.

Example: XPS and XAS studies of electrochemically formed oxides on Al-Cr alloys

This section summarizes work we have recently carried out, in collaboration with others, on the use of XPS and XAS to study the composition of electrochemically formed surface oxide films on Al–Cr alloys. Interested readers may find more details in [33–36]. It will be shown that, while XPS provided considerable insight, the use of XAS was extremely useful. The presence of a sharp pre-edge peak associated with Cr⁺⁶ makes this technique particularly sensitive for the detection of Cr in its highest valence state. Furthermore, *in situ* XAS measurements carried out in aqueous solution with samples under potential control were very instructive.

The chemical state of Cr in passive oxide films is of interest because of the corrosion resistance it imparts as an alloying element. Whereas the equilibrium solubility of Cr

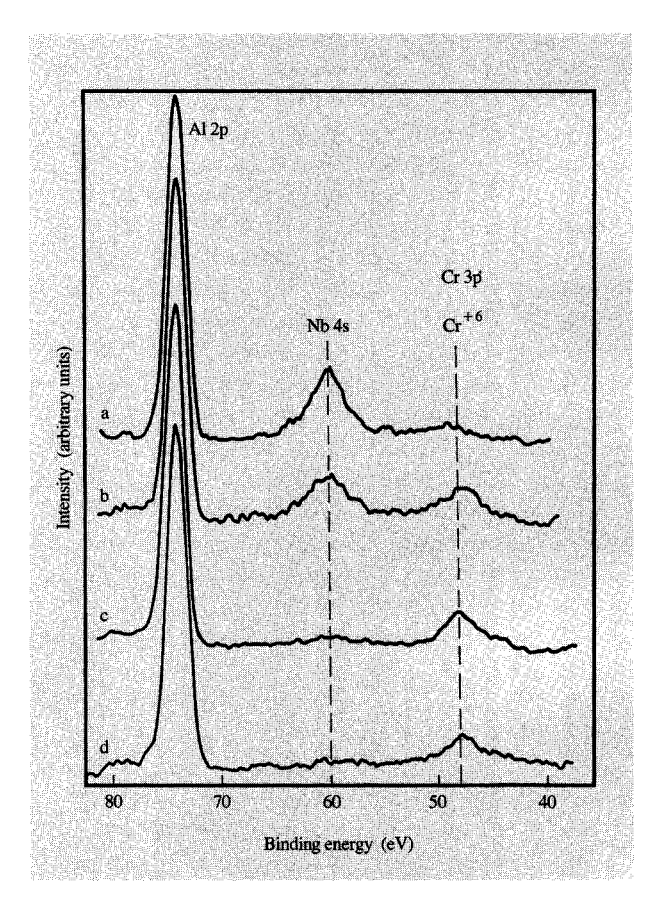


Figure 5

XPS spectra for 40-Å-thick Al-Cr films polarized to 5 V vs. MSE. The bulk compositions of the films were 5%, 20%, 32%, and 43% Cr, as shown by curves a-d, respectively. The spectra were normalized as in Figure 4. From [33], reprinted by permission of the publisher, The Electrochemical Society, Inc.

in Al is extremely small, it has recently been shown that large amounts of Cr and other alloying elements in Al remain in solid solution for thin films prepared by vapor deposition techniques [37, 38]. The films in this study were sputter-deposited onto several different substrates: quartz for XPS studies, float glass for XPS and $ex\ situ\ XAS$ studies, and Mylar for $in\ situ\ XAS$ studies. Most of the Al–Cr films examined were 20 or 40 Å thick and had a 1000–2000-Å-thick underlying layer of Nb or Ta. The electrolyte was 0.5 M $H_3BO_3+0.05\ M\ Na_2B_4O_7$ with a pH of 7.4. A mercurous sulfate reference electrode was used (MSE, 0.64 vs. standard hydrogen electrode); all potentials are referred to the MSE scale.

The Al 2p and Cr 3p XPS peaks for 40-Å-thick, as-deposited, ambient-exposed alloy samples are shown in **Figure 4**; the energy was corrected for charging by using the adventitious C peak at 284.6 eV. The Cr concentrations determined from the Cr/Al XPS area ratios (oxidized + metallic) were lower than the bulk values determined by Rutherford backscattering. This indicated that the Cr in the alloy tends to be protected by preferential surface segregation and oxidation of Al.

The Al and Cr metallic peaks shift to higher binding energy as the Cr concentration increases. This observation may be explained by charging, which is observed even for thin oxides on metals during photoemission. As a result of this charging, the potentials of the oxide and the adventitious C on the oxide surface (used as a reference) are more positive than the underlying metal, which is electrically connected to the spectrometer and is therefore not charged. The ratio of metallic to oxidized peak heights decreases for both Al and Cr as the Cr concentration decreases, indicating the presence of a thicker oxide film. Since thicker oxide films can sustain a larger charge, the referencing method used results in an apparent shift toward lower binding energies for the metallic components of both Cr and Al as the Cr concentration decreases. This shift is an artifact and not representative of a true shift in binding energy resulting from alloying [28]. However, it illustrates one of the problems associated with XPS data interpretation.

The XPS spectra obtained after polarization of the alloy samples at 5 V are shown in **Figure 5**. These spectra exhibited a Cr 3p peak at 48 eV. Comparison with the XPS database [23] indicated that the Cr in the oxides was primarily in the 6+ oxidation state. **Figure 6** shows the effect of polarization potential for 40-Å-thick Al-43% Cr films. Oxidation state and oxide thickness increase with potential. The shoulder at 48 eV in curve a of Figure 6 and curve d of Figure 4 resulted from a satellite of the 3p peak of Cr⁺³, and not from Cr⁺⁶. This was verified by analysis of the corresponding Cr 2p peaks, which are not shown. Samples polarized at or above 0.7 V exhibited Cr 3p peaks corresponding to the 6+ oxidation state that were roughly

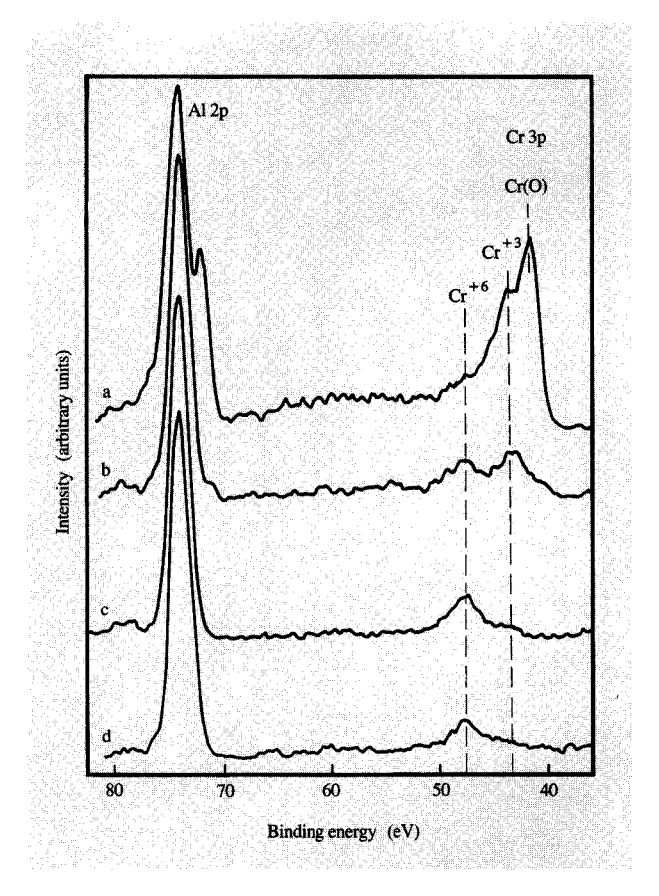


Figure 6

XPS spectra for 40-Å-thick 43% Cr films polarized at -0.5 V vs. MSE (curve a), 0.7 V vs. MSE (curve b), 2 V vs. MSE (curve c), and 5 V vs. MSE (curve d). The spectra were normalized as in Figure 4. From [33], reprinted by permission of the publisher, The Electrochemical Society, Inc.

equivalent in area. A similar area was found for the spectra shown in Figure 5. The total amount of Cr⁺⁶ was apparently independent of potential and alloy composition.

As just described, XPS analysis provided information regarding the composition of the oxide films, the valency distribution, and the relative concentrations of their components. It was found that considerable amounts of Cr⁺⁶ remained in the films at high potentials despite the large solubility of the chromate ion. More information about the nature of Cr⁺⁶ in the films was generated from the Cr LVV Auger peak, which could be observed during XPS analysis. This Auger peak is much more sensitive than either XPS or XAS to the exact bonding structure of Cr⁺⁶. Illustratively, Figure 7 shows Cr LVV Auger spectra for Cr metal and various Cr oxides. Cr⁺⁶ in oxides formed electrochemically on Al-Cr films was compared to Cr⁺⁶ adsorbed from chromate solution onto anodized Al.



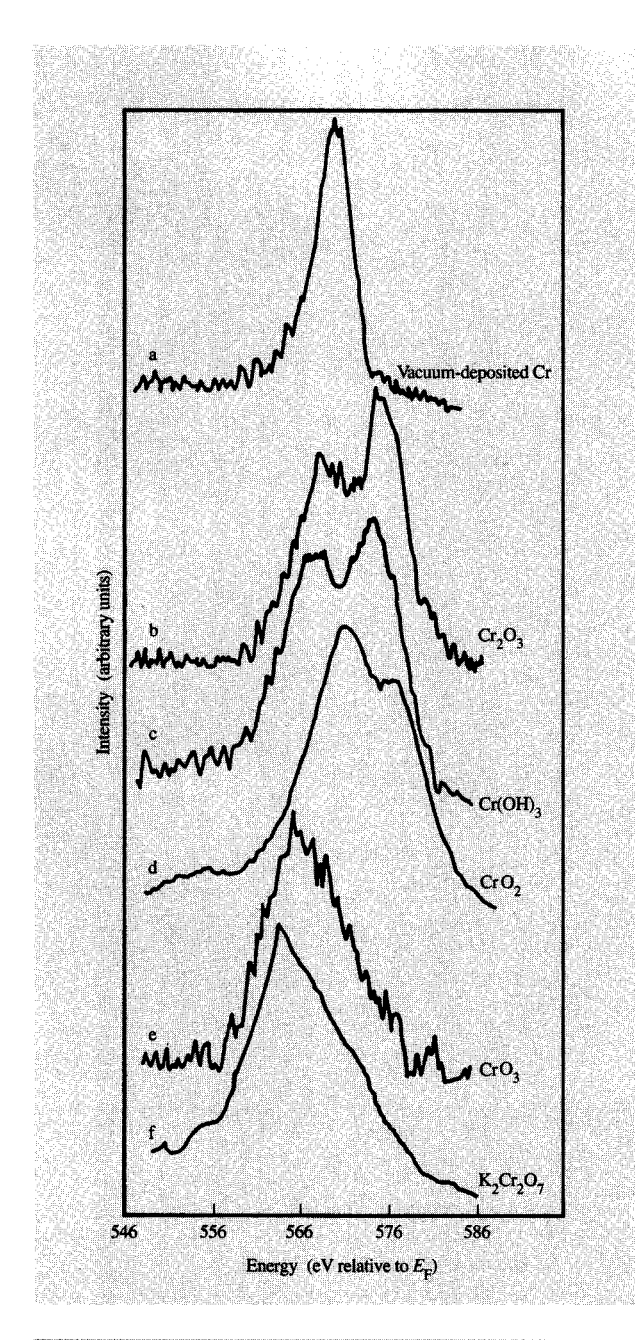


Figure 7

Cr LVV Auger spectra for *in situ* vacuum-deposited Cr (curve a), Cr_2O_3 powder (curve b), $Cr(OH)_3$ powder (curve c), CrO_2 powder (curve d), CrO_3 powder (curve e), and $K_2Cr_2O_7$ powder (curve f). From [35], reprinted with permission.

Figure 8 shows that the Cr⁺⁶ ions adsorbed on the anodized Al behaved like chromate ion (see curve f in Figure 7); namely, screening charge was easily transferred from the oxygen ligand in the final state of the photoemission process. This charge transfer from the ligand allowed the Cr LVV Auger transition to occur from

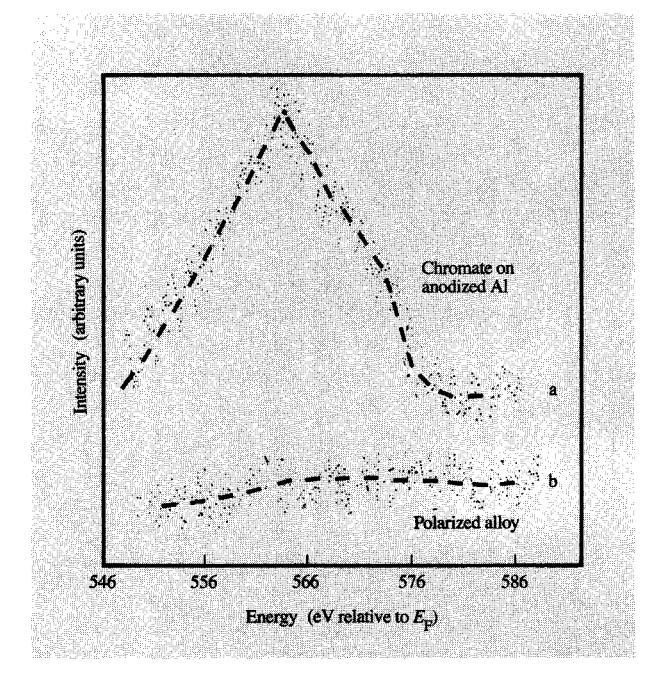


Figure 8

Cr LVV Auger spectra for adsorbed chromate on an anodized Al film (curve a) and Al-43% Cr film polarized at 5 V vs. MSE (curve b). The dashed lines have been added to aid the reader, since the signals were weak. From [35], reprinted with permission.

the nominally empty d band, and the structure was found to be susceptible to radiation-induced decomposition. On the other hand, for the Cr⁺⁶ in oxides on the Al-Cr films, screening charge is not readily transferred from the oxygen ligand. As a result of this and the fact that the d band for Cr⁺⁶ is nominally empty, the Cr LVV Auger transition was not possible and was not observed. Correspondingly, Cr⁺⁶ in the oxides on Al-Cr alloys did not readily suffer photodecomposition. This implies that the Cr-O bond for this Cr⁺⁶ in the alloy oxide is affected by the influence of the second nearest neighbor, Al. As a result, the Cr⁺⁶ behaves as if integrated into the oxide structure and is not isolated as chromate anions. This is consistent with the observation described below that the Cr in the oxide is electroactive and can change coordination during oxidation and reduction cycles.

XAS studies were performed on Al-Cr films using two configurations. Ex situ measurements in the glancing-angle mode were made on samples that had been pretreated in a cell to form an oxide film. For in situ experiments, use was made of a configuration described previously in which the metal film was deposited on a Mylar window. Transmission absorption measurements carried out on Cr reference standards at the Cr K edge are shown in

Figure 9. The absorption edge moves monotonically to higher energies with increasing oxidation state. A pre-edge peak associated with Cr⁺⁶ is clearly evident. Shown in Figures 10 and 11 are absorption edges, measured *ex situ*, for samples that were similar to those of Figures 5 and 6. The edges were normalized to the total amount of Cr in each sample; hence, they only reveal the proportions of the various Cr oxidation states. As can be seen, the pre-edge peak was the predominant feature in the results obtained, and the amount of Cr⁺⁶ and the absorption edge energy were found to increase with potential for 20% Cr films, and with Cr concentration for films polarized at 2 V. These trends matched those determined by the XPS analyses.

Systematic oxidation at a high potential, reduction at a low potential, and reoxidation indicated that the Cr in the oxide films was electroactive. This characteristic was examined with the *in situ* configuration, and the results are shown in **Figure 12** with spectra of reference standards indicated by the dotted curves. These measurements were carried out while the sample was in solution and under potential control. At open circuit (curve a), the Cr was

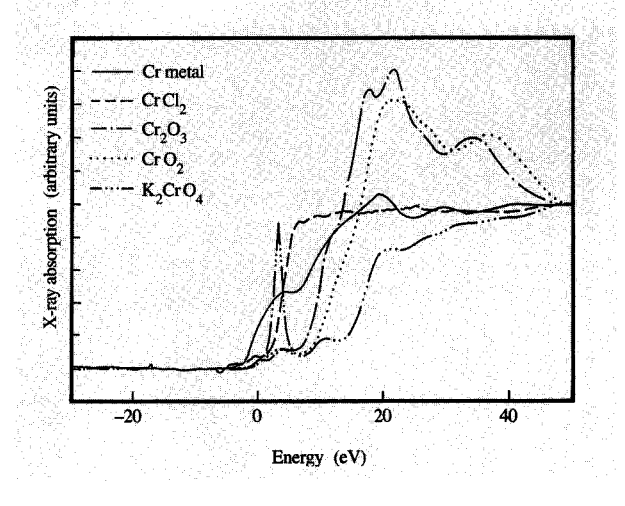


Figure 9

Adsorption edges of reference standards relative to the Cr K edge at 5989 eV. From [33], reprinted by permission of the publisher, The Electrochemical Society, Inc.

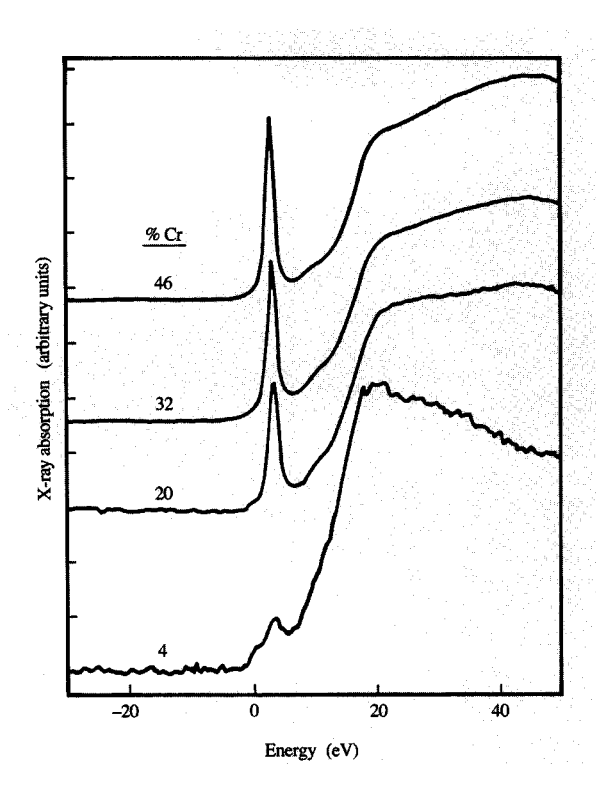


Figure 10

Influence of alloy composition on absorption edges for 40-Å-thick Al-Cr films polarized at 2 V vs. MSE, measured below the critical angle. From [33], reprinted by permission of the publisher, The Electrochemical Society, Inc.

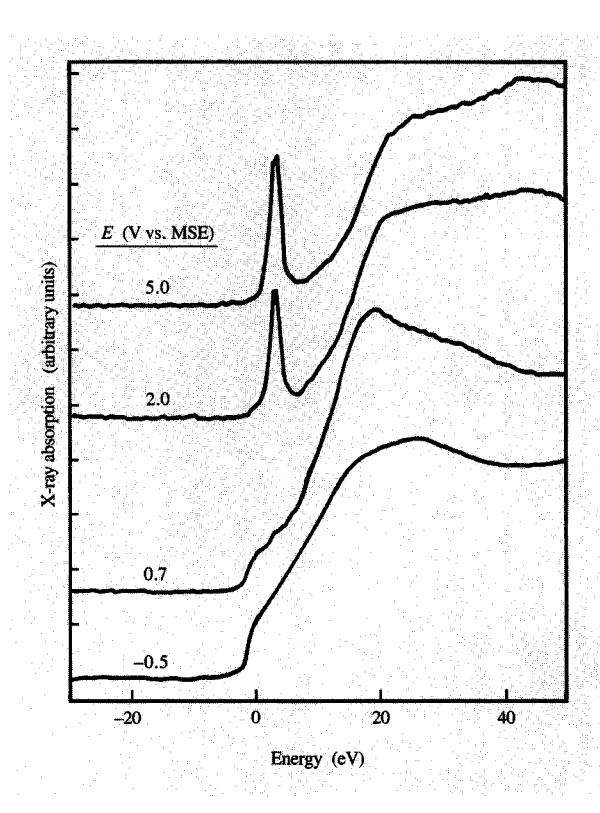


Figure 11

Influence of applied potential on absorption edges for 40-Å-thick Al-Cr films containing 20% Cr, measured below the critical angle. From [33], reprinted by permission of the publisher, The Electrochemical Society, Inc.

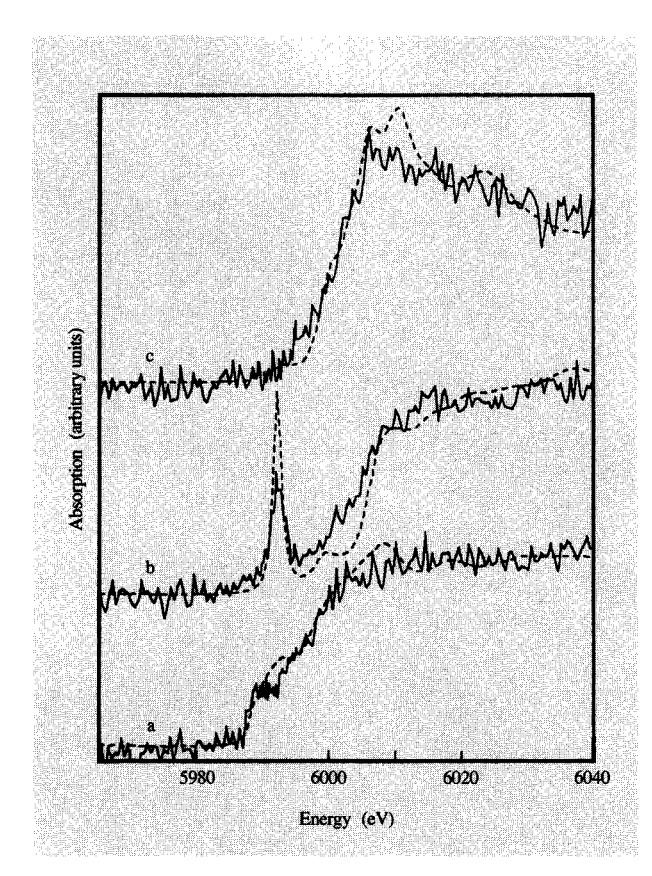


Figure 12

In situ XAS measurement of the Cr K edge of a 20-Å-thick Al-12% Cr film at open circuit (curve a), after seven minutes at 2 V vs. MSE (curve b), and after six minutes at -1.5 V vs. MSE (curve c), as shown by solid lines. The broken lines show standard compounds measured in transmission: Cr metal (curve a), $\rm K_2CrO_4$ (curve b), and $\rm Cr_2O_3$ (curve c). From [34], reprinted by permission of the publisher, The Electrochemical Society, Inc.

predominantly in the metallic state, since the oxidized Al segregated to the surface protected it. From the height of the pre-edge peak and the edge position, the oxidation state of Cr during the polarization to 2 V (curve b) could be estimated to be 50% in the 6+ state and 50% in the 3+ state. Reduction at -1.5 V (curve c) reduced the Cr⁺⁶, since all of the Cr was found to be in the 3+ state. The Cr could subsequently be cycled between the 6+ and 3+ states by appropriate potential treatments. The Cr⁺⁶ was found to be stable in the oxide if the potential was increased to a high value in one step from the open circuit value.

Figure 13 shows that the situation is different if the potential is increased in 100-mV steps. The spectra in this figure were collected with coarse energy increments and a short counting time per point in order to minimize the total spectrum collection time to 3 min. Data not shown indicated that from -0.7 V to -0.3 V the Cr is metallic,

and at about -0.2 V there is a transition to Cr^{+3} , which persists until +0.1 V. At +0.2 V the characteristic Cr⁺⁶ pre-edge peak appears and dissolution is significant, as indicated by the decrease in edge heights (the in situ spectra were not normalized). Comparison of Figures 12 and 13 shows that, during slow polarization of Al-Cr through +0.2 V, Cr dissolves via formation of chromate, and that if the potential is stepped directly to a high value, the Cr is trapped in the film as Cr +6. Other experiments indicated that, once Cr⁺⁶ is trapped in the film at a high potential, subsequent stepping of the potential through the critical potential of 0.2 V in small steps does not result in dissolution. Pure Cr films were also found to dissolve rapidly at 0.2 V in a manner similar to the Al-Cr alloys. However, pure Cr dissolved even when the potential was jumped directly to a high value.

The kinetics of the oxidation reaction to Cr⁺⁶ upon jumping of the potential were also studied *in situ*. **Figure 14** shows the edges observed for an Al-12% Cr film prior to and following stepping of the potential to 2.0 V.

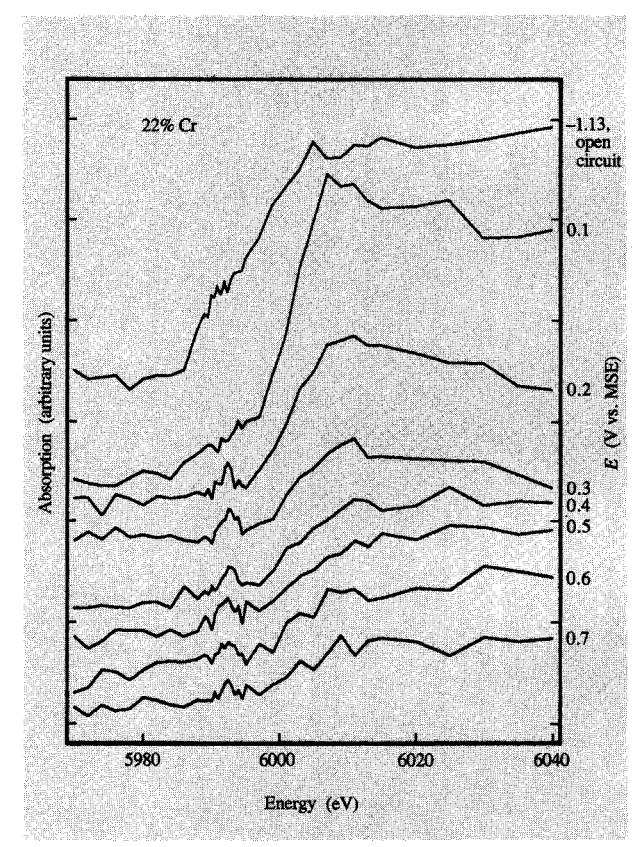


Figure 13

Cr K edge for a 20-Å-thick A1-22% Cr film polarized at the potentials indicated. From [36], reprinted by permission of the publisher, The Electrochemical Society, Inc.

The fast spectra taken during the first minutes at 2 V indicated that the Cr changes quickly from metallic to Cr⁺³. Only during a slower 30-min scan does the pre-edge peak associated with Cr⁺⁶ appear and stabilize.

While in this example the ex situ XAS data generated little understanding beyond that obtained by XPS, the preedge peak unambiguously indicated the presence of Cr⁺⁶. Interpretation of the XPS data is straightforward when all of the Cr is present as Cr +6, as in Figure 5. However, when a mixture of oxidation states is present and Cr⁺⁶ is represented as a small shoulder, deconvolution is difficult and interpretation of the data is fraught with risk [37]. In contrast, the distinct pre-edge peak associated with Cr⁺⁶ permits the identification of even a small amount of Cr+6 in a mixture with other oxidation states, as shown, for instance, in Figure 14. Furthermore, the in situ XAS experiments carried out under potential control provided the capability to perform a relatively rapid analysis of a dynamic system under well-controlled conditions. The effect of polarization rate on Cr behavior could have been found using ex situ experiments only, but that would have been much more difficult. Observation of the kinetics of the transformations was only possible with the in situ technique.

The XAS experiments, however, were clearly limited because of the inability to monitor the behavior of Al in the same experiment. The K edge of Al at 1560 eV is below the range that can be achieved with most hard X-ray beam lines. The same applies to oxygen. It should be noted that the Al and O edges are accessible using soft X-rays. Their low energy, however, precludes the possibility of *in situ* experiments. In contrast to XAS, XPS could be used to obtain information on the Al, Cr, O, C, and also the Nb underlayer that was used. Information on the behavior of these elements was critical for a complete understanding of the system. Finally, the use of the Cr LVV Auger peak made it possible to detect effects that XPS and XAS could not be used to detect. The combined use of all of these techniques was needed.

Concluding remarks

We have attempted to underscore the advantages of the coordinated use of XPS and XAS for the study of electrochemically formed oxide films. While it may be time-consuming, combining these techniques provides a unique insight to the study of the properties of passive films and is potentially very rewarding. A brief description has been included of the fundamental processes involved and of the capabilities and limitations of the techniques when applied to electrochemical studies.

Acknowledgments

The authors would like to thank A. J. Davenport, H. S. Isaacs, C. V. Jahnes, and M. A. Russak for significant contributions to aspects of the work.

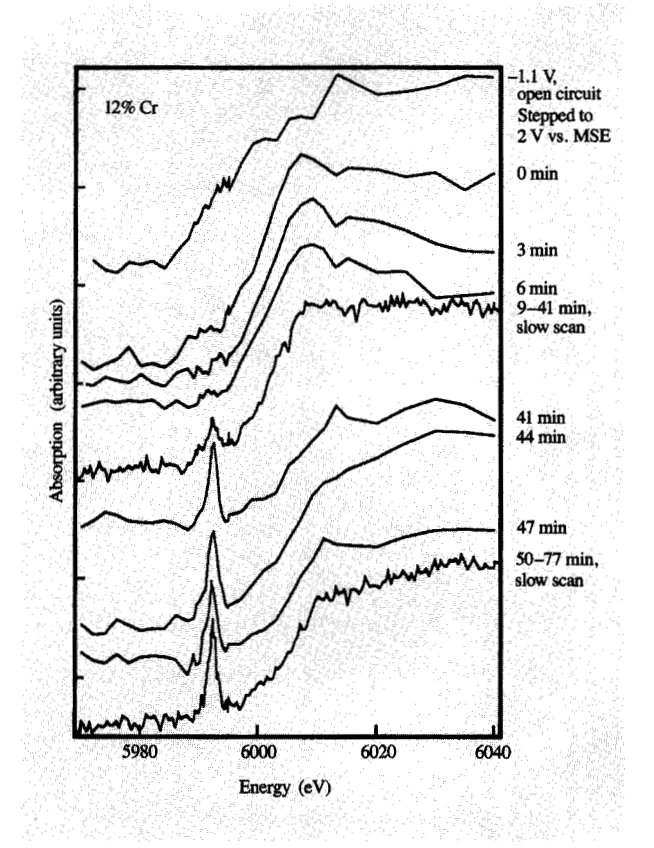


Figure 14

Cr K edge for a 40-Å-thick Al-12% Cr alloy. The potential was stepped from open circuit to 2 V vs. MSE. The indicated times are the times elapsed between the stepping and the start of collection of each spectrum. From [36], reprinted by permission of the publisher, The Electrochemical Society, Inc.

References

- J. Kruger, in Critical Factors in Localized Corrosion, G. S. Frankel and R. C. Newman, Eds., The Electrochemical Society, Pennington, NJ, 1992, PV 92-9, p. 184.
- G. C. Allen, P. M. Tucker, A. Capon, and R. Parsons, J. Electroanal. Chem. 50, 335 (1974).
- 3. J. Olefjord, Corros. Sci. 15, 687 (1975).
- J. S. Hammond and N. Winograd, J. Electroanal. Chem. 78, 55 (1977).
- N. S. McIntyre and J. C. Riviere, in *Practical Surface Analysis*, D. Briggs and M. P. Seah, Eds., John Wiley & Sons, New York, 1983, p. 6.
- G. G. Long, J. Kruger, D. R. Black, and M. Kuriyama, J. Electroanal. Chem. 150, 603 (1983).
- A. J. Forty, M. Kerkar, J. Robinson, and M. Ward, J. de Phys. 47, C8-1077 (1986).
- G. G. Long, J. Kruger, and D. Tanaka, J. Electrochem. Soc. 134, 264 (1987).
- J. K. Hawkins, H. S. Isaacs, S. M. Heald, J. Tranquada, G. E. Thompson, and G. C. Wood, *Corros. Sci.* 27, 391 (1987).

- Photoemission in Solids, Vols. I and II, M. Cardona and L. Ley, Eds., Springer-Verlag, Berlin, 1979.
- X-Ray Absorption: Principles, Applications, Techniques of EXAFS, SEXAFS and XANES, D. C. Koningsberger and R. Prins, Eds., John Wiley & Sons, New York, 1988.
- 12. T. Koopmans, Physica 1, 104 (1933).
- D. A. Shirley, in *Photoemission in Solids*, Vol. I, M. Cardona and L. Ley, Eds., Springer-Verlag, Berlin, 1979, p. 186.
- D. Briggs and J. C. Riviere, in *Practical Surface Analysis*,
 D. Briggs and M. P. Seah, Eds., John Wiley & Sons, Inc.,
 New York, 1983, p. 88.
- K. Siegbahn, ESCA: Atomic, Molecular, and Solid State Structure Studied by Means of Electron Spectroscopy, Almquist and Wiksells, Upsala, Sweden, 1967.
- 16. A. Rosencwaig and G. K. Wertheim, J. Electron. Spectrosc. 1, 493 (1973).
- A. Bianconi, in X-Ray Absorption: Principles, Applications, Techniques of EXAFS, SEXAFS and XANES, D. C. Koningsberger and R. Prins, Eds., John Wiley & Sons, Inc., New York, 1988, p. 573.
- S. Sugano, Y. Tanabe, and H. Kamimura, Multiplets of Transition Metal Ions in Crystals, Academic Press, Inc., New York, 1970.
- J. C. Riviere, in *Practical Surface Analysis*, D. Briggs and M. P. Seah, Eds., John Wiley & Sons, Inc., New York, 1983, p. 17.
- W. M. Riggs and M. J. Parker, in Methods of Surface Analysis, A. W. Czanderna, Ed., Elsevier, New York, 1975, p. 123.
- 21. A. T. Hubbard, J. Vac. Sci. Technol. 17, 49 (1980).
- D. Aberdam, R. Durand, R. Faure, and F. El-Omar, Surf. Sci. 171, 303 (1986).
- NIST X-ray Photoelectron Spectroscopy Database (Standard Reference Data Program), C. D. Wagner, Ed., U.S. Dept. of Commerce, Washington, DC, 1989.
- A. J. Davenport and H. S. Isaacs, in Surface and Interface Characterization in Corrosion, S. Shah, Ed., National Association of Corrosion Engineers, Houston, 1992, in press.
- H. D. Abruna, in Modern Aspects of Electrochemistry, Vol. 20, J. O'M. Bockris, R. E. White, and B. E. Conway, Eds., Plenum Press, New York, 1989, p. 265.
- 26. H. Chen and S. M. Heald, Phys. Rev. B 42, 4913 (1990).
- M. Kerkar, J. Robinson, and A. J. Forty, Faraday Discuss. Chem. Soc. 89, 31 (1990).
- D. A. Stephenson and N. J. Binkowski, J. Non-Cryst. Solids 22, 399 (1976).
- D. K. G. de Boer, C. Haas, and G. A. Sawatzky, *Phys. Rev. B* 53, 2518 (1984).
- D. M. Kolb and R. Michaelis, J. Electroanal. Chem. 284, 507 (1990).
- R. W. Hoffman, in Passivity of Metals and Semiconductors, M. Froment, Ed., Elsevier, Amsterdam, 1983, p. 147.
- G. G. Long and J. Kruger, in Techniques for the Characterization of Electrodes and Electrochemical Processes, R. Varma, Ed., John Wiley & Sons, Inc., New York, 1991, p. 167.
- G. S. Frankel, A. J. Davenport, H. S. Isaacs, A. G. Schrott, C. V. Jahnes, and M. A. Russak, J. Electrochem. Soc. 139, 1812 (1992).
- A. J. Davenport, H. S. Isaacs, G. S. Frankel, A. G. Schrott, C. V. Jahnes, and M. A. Russak, J. Electrochem. Soc. 138, 337 (1991).
- A. G. Schrott, G. S. Frankel, A. J. Davenport, H. S. Isaacs, C. V. Jahnes, and M. A. Russak, *Surf. Sci.* 250, 139 (1991).
- A. J. Davenport, H. S. Isaacs, G. S. Frankel, A. G. Schrott, C. V. Jahnes, and M. A. Russak, in X-Ray Methods in Corrosion and Interfacial Electrochemistry,

- A. J. Davenport and J. Gordon, Eds., The Electrochemical Society, Pennington, NJ, 1992, PV 92-1, p. 261.
- W. C. Moshier, G. D. Davis, and G. O. Cote, J. Electrochem. Soc. 136, 356 (1989).
- G. S. Frankel, C. V. Jahnes, M. A. Russak, M. Mirzamaani, and V. A. Brusic, J. Electrochem. Soc. 136, 1243 (1989).

Received January 21, 1992; accepted for publication September 17, 1992

Alejandro G. Schrott IBM Research Division, Thomas J. Watson Research Center, P.O. Box 218, Yorktown Heights, New York 10598 (SCHROTT at WATSON, schrott@watson.ibm.com). Dr. Schrott is a Research Staff Member in the Manufacturing Research Department at the Thomas J. Watson Research Center. He carried out his undergraduate work at the University of Buenos Aires, Argentina, and received a Ph.D. degree in physics from the University of Washington in 1982. He subsequently worked as a Postdoctoral Associate in the Department of Materials Sciences, Cornell University. In 1984, Dr. Schrott joined IBM at the Thomas J. Watson Research Center, where he has worked on surface and interfacial properties of metal-insulator systems.

Gerald S. Frankel IBM Research Division, Thomas J. Watson Research Center, P.O. Box 218, Yorktown Heights, New York 10598 (GSFRANK at WATSON, gsfrank@watson.ibm.com). Dr. Frankel is a Research Staff Member in the Manufacturing Research Department at the Thomas J. Watson Research Center. He received an Sc.B. degree in materials science from Brown University in 1978. After working at Arthur D. Little, Inc. for two years, he attended the Massachusetts Institute of Technology and received an Sc.D. degree in materials science and engineering in 1985. He subsequently carried out postdoctoral research for one year at the Swiss Federal Technical Institute in Zurich. In 1986, Dr. Frankel joined IBM at the Thomas J. Watson Research Center, where he has primarily been studying the corrosion of thin films used in magnetic storage and electronic applications. He is a member of The Electrochemical Society.